Observation of Laser Driven Supercritical Radiative Shock Precursors

S. Bouquet,[1] C. Stéhlé,[2] M. Koenig,[3] J.-P. Chièze,[4] A. Benuzzi-Mounaix,[3] D. Batani,[5] S. Leygnac,[2] X. Fleury,[1] H. Merdji,[6] C. Michaut,[2] F. Thais,[4,6] N. Grandjouan,[3] T. Hall,[7] E. Henry,[3,5] V. Malka,[3] and J.-P. J. Lafon[8]

[1]*Département de Physique Théorique et Appliquée (DPTA), CEA-DIF, BP 12, 91680 Bruyères-le-Châtel, France*
[2]*Laboratoire de l'Univers et de ses Théories (LUTH), Observatoire de Paris, 92195 Meudon, France*
[3]*Laboratoire pour l'Utilisation des Lasers Intenses (LULI), CNRS–CEA–Université Paris VI–Ecole Polytechnique, 91128 Palaiseau, France*
[4]*Service d'Astrophysique (SAp), CEA–Saclay, DSM/DAPNIA, 91191 Gif-sur-Yvette cedex, France*
[5]*Dipartimento di Fisica "G. Occhialini," Università di Milano-Bicocca and INFM, Piazza della Scienza 3, 20126 Milano, Italy*
[6]*Service Photons Atomes et Molécules (SPAM), CEA–Saclay, DSM/DRECAM, 91191 Gif-sur-Yvette cedex, France*
[7]*University of Essex, Colchester CO4 3SQ, United Kingdom*
[8]*Galaxies, Etoiles, Physique et Instrumentation (GEPI), Obervatoire de Paris, 92195 Meudon Cedex, France*

(Received 5 June 2002; published 2 June 2004)

We present a supercritical radiative shock experiment performed with the LULI nanosecond laser facility. Using targets filled with xenon gas at low pressure, the propagation of a strong shock with a radiative precursor is evidenced. The main measured shock quantities (electronic density and propagation velocity) are shown to be in good agreement with theory and numerical simulations.

DOI: 10.1103/PhysRevLett.92.225001 PACS numbers: 52.72.+v, 95.30.Jx

Radiative hydrodynamic processes [1–3] are very important in inertial confinement fusion [4] and astrophysics [1,5–7]. Recent experiments have reproduced hydroradiative astrophysical flows (jets or blast waves) [8–14] and radiative shocks (RS) [15–19]. In most astrophysical environments, such as envelopes of post-asymptotic giant branch stars, a RS is characterized by (1) an ionized precursor, ahead of the shock, heated by radiation coming from the high temperature shocked gas, (2) a shock front followed by a short extension region where relaxation between ions, electrons, and photons takes place, and (3) a recombination zone in the downstream flow. In the vicinity of the shock and, provided its velocity D is larger than $D_{\rm cr}$, the precursor is heated up to a temperature $T_{\rm cr}$ equal to that of the shocked gas. Shocks satisfying $D > D_{\rm cr}$ are called "supercritical" (SC) [1,3] and their structures are very sensitive to the treatment of radiation transport and to its coupling with hydrodynamics. Consequently, laboratory experiments [8–19] are very relevant test beds for validating models and theoretical predictions.

The critical velocity ($D_{\rm cr}$) above which a RS enters the SC regime is the solution of the implicit equation [1,3] $\sigma[T_{\rm cr}(\rho_1, D_{\rm cr})]^4 = \rho_1 D_{\rm cr} \varepsilon[\rho_1, T_{\rm cr}(\rho_1, D_{\rm cr})]$, where $\varepsilon(\rho, T)$ is the internal energy, per unit mass, of the fluid (mass density ρ_1) ahead of the shock. This steady relation assumes that the photon flux emerging at the shock front is entirely absorbed to ionize and to heat, up to the post shock temperature, the unperturbed gas ahead.

In this Letter, new aspects of the RS are raised compared to previous published results [8–19]. Radiative precursors have also been produced earlier [9,13,14,16,19]; however, regimes differ from the one we get. The goals differ also on at least two points. First, most of the former experiments deal with gas jets containing atomic clusters [9,14,19]. They are rapidly heated by the laser beam and the radiation they emit propagates ahead of the shock, producing a photoionized precursor mostly not heated since the very low density medium let the radiation escape (in our case, it is heated up to $\sim$15 eV). Second, Taylor-Sedov blast waves, i.e., shock waves created by instantaneous, zero spatial extension explosions, are produced [9,13,14,16]. While it is propagating, the shock decays rapidly since no more energy is supplied. Moreover, the blast wave generates an inner cavity with a decreasing mass density. In our study, energy is continuously injected (piston with velocity V_p) in the wave and the material is highly compressed behind the shock. This is quite the opposite of the blast wave evolution.

In this Letter we present measurements of the velocity U_p and ionization of the precursor of a SC-RS and they are compared to simulations. In order to strengthen radiative effects against thermal ones, a low-density medium with a high atomic mass is prescribed, and xenon gas at 0.1 and 0.2 bar (1 order of magnitude lower than in Ref. [15]) is chosen. Using a screened hydrogenic-type equation of state (EOS) for Xe and taking an initial density $\rho_1 = 10^{-3}$ g/cm^3, the critical velocity is as low as $D_{\rm cr} \sim 15$ km/s, leading to $T_{\rm cr} \sim 7$ eV. This low $D_{\rm cr}$ is partly due to the large heat capacity of Xe. Former experiments at LULI have shown that shock with $D \sim 50$ km/s in low-density media are achievable with the nanosecond laser facility [20] and it is, therefore, quite suitable to generate RS in low-density Xe gas.

Experiments are performed in small, millimeter size targets and the shock is far from equilibrium, at least regarding its radiative properties. The length L of a stationary precursor generated by a shock with a constant velocity D can be derived by equating the diffusion time

of photons (mean free path λ) across the precursor to the time for the material to cover L. One gets $L \sim \lambda c/D$ (c is the velocity of light) and, for the present experiments, $L \sim 1$ m. The corresponding equilibrium time is of the order of L/D, i.e., tens of microseconds. A time-dependent model based on self-similar solutions of the nonlinear heat equation [17] shows that in the transient phase the length $l(t)$ of the precursor grows up to L according to the law $l(t) = 8.7 \times 10^{-7}\ [\rho_1(\mathrm{kg/m^3})]^{11/36} \times (D[\mathrm{m/s}])^{13/6} \times (t[s])^{31/36}$; $l(t)$ is in meters. For $D = 65$ km/s and $\rho_1 = 10^{-3}$ g/cm^3, we obtain $l \sim 1$ m for $t = 10$ μs, in agreement with the above result. In addition, according to the Xe shock adiabat, the compression rate ρ_2/ρ_1 achieved for this shock velocity is about 11 in an idealized situation (planar geometry). This result assumes a stationary RS with $D = \mathrm{const}$ and a precursor with constant length L. However, at earlier time the precursor grows and the value of the radiation flux should be larger than its stationary value. Indeed, in the stationary regime, the energy supplied by the flux is used only to maintain the propagation of the precursor (heating and ionization) while in the early transient phase the flux should provide energy for both its propagation plus its growth, until the steady state can be obtained. In the transient stage, more energy than in the steady one is radiated ahead of the discontinuity and, consequently, the temperature of the shocked gas is lower than in the final state with a compression rate larger than 11, depending on the magnitude of the emissivity. This property explains, to some extent, the high compressions achieved by strong shocks propagating in optically thin media.

The design of the experiment has been carried out with the radiation hydrocodes MULTI [21] and FCI [22] (CEA code). A RS is produced at ~100 J of pulsed laser light. A three-layer pusher drives the shock into the Xe gas initially at rest in a quartz cell (~1 mm^3 volume). This pusher is made of a polyethylene ablator (2 μm), a titanium x-ray screen (3 μm), and a polyethylene foam accelerator (25 μm). The laser beams focus on the ablator and the foam/Xe interface acts as a piston moving at $V_p \sim 70$ km/s. This high velocity produces the RS together with its radiative precursor (Fig. 1).

Experiments have been carried out using three of the six available beams of the LULI's Nd-glass laser. The beams were converted at $\lambda = 0.53$ μm, providing a maximum total energy $E_{2\omega} \approx 100$ J focused in a 500 μm [full width at half maximum (FWHM)] diameter spot with a 250 μm flat center. The spatially averaged intensity is ~4–6 $\times 10^{13}$ W/cm^2 depending upon the laser energy. The laser square pulse has a 120 ps rise time with a 720 ps FWHM. Each beam is focused with a 500 mm lens and phase zone plates [23] are used to remove large-scale spatial modulations and to obtain a uniform intensity in the spot [24].

The experimental diagnostics are shown in Fig. 2. They focus on the time-dependent properties of the precursor.

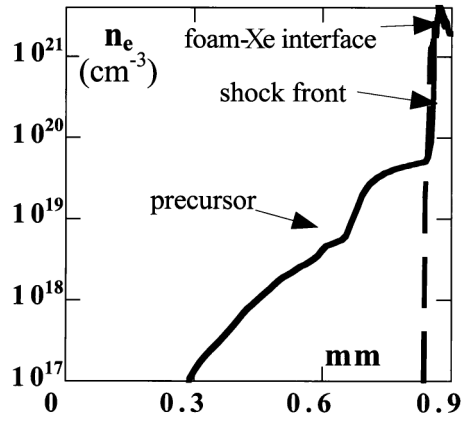

FIG. 1. MULTI simulations [21] ($I = 6 \times 10^{13}$ W cm^{-2}) with and without radiation (dashed and solid curve, respectively).

A streak camera records the self-emitted light from the rear surface of the target at shock breakout and two velocity interferometer systems for any reflector (VISARs) [25] with different sensitivities (16.63 and 3.39 km/s per fringe) measure D in the foam or in the gas provided the electron density n_e becomes overcritical. Finally, a Mach-Zehnder interferometer provides n_e along the shock propagation. Two streak cameras are used, one looking at the fringes longitudinally (LONG), the other giving a transverse image at a given position in the xenon (TRANS). Assuming a transverse plasma thickness ~200 μm, a range $n_e = 10^{18}$–10^{20} cm^{-3} in the precursor is inferred from the interferometer. With the VISAR, we measure V_p (foam/gas interface, i.e., piston) provided the gas remains transparent to the probe laser light. As we can see in Fig. 3, the fringes shift first to the left (velocity jump due to a slight deceleration), then to the right (small acceleration), and finally back to the left. The mean measured shock velocity is $D \sim 67$ km/s, i.e., $D \sim 4D_{\mathrm{cr}}$. In addition to the fact that numerical simulations show a shock with a precursor (Fig. 1), the computed velocities are in good agreement with this experimental value. The above three stages correspond to a first shock breaking through the foam-Xe interface, then a second shock arrives (due to reflections on the pusher interfaces) and catches the first one and, finally, the piston decelerates slowly (see below).

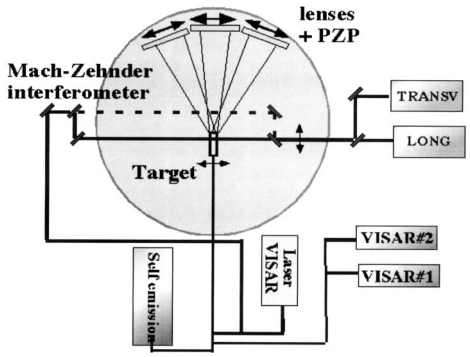

FIG. 2. Experimental setup and diagnostics.

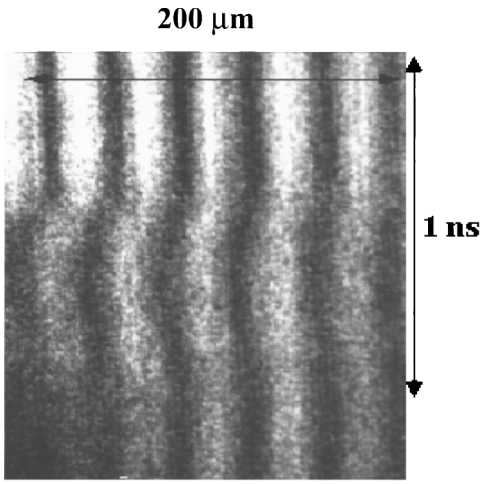

FIG. 3. VISAR image for a 0.2 bar filled gas cell.

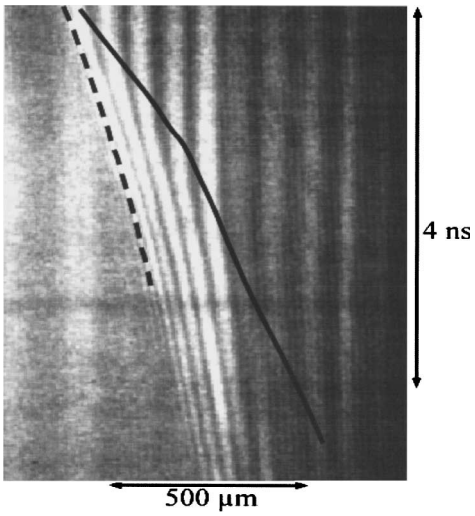

FIG. 4. Interferometry (LONG) in Xe gas. The dashed (solid) line defines the shock (precursor) front trajectory.

According to the expected shock temperature ($T_2 \sim 20$ eV) and the associated ionization state, the shock front in Xe is overcritical ($n_e \approx 10^{21}$ cm^{-3}) while the precursor is much less than critical ($n_e \leq 10^{20}$ cm^{-3}); see Fig. 1. The Mach-Zehnder interferometer pattern (Fig. 4) shows two different perturbations propagating in the gas. The first (dashed curve) separates the region where n_e is overcritical (left side of the curve) from the zone in the rear part of the cell where n_e is subcritical. It corresponds to the shock front and we can deduce D again. For the first 0.4 ns, it is 68 km/s and decays down to 60 km/s when averaged over the first 3 ns. This value is very close to the VISAR measurement (67 km/s). After $t \approx 3$ ns, it slows down since the laser pulse is only $\sim$1 ns long. In Fig. 4 we also clearly observe fringe shifts (solid line) due to a change in n_e ahead of the shock. We associate the zone in between the two lines with the precursor and the solid curve gives the position of its front. In accordance with the analytical expression for $l(t)$, the precursor grows roughly linearly with t. Over the first 2 ns, its velocity (slope of the solid line) is $U_p \sim 130$ km/s, i.e., $U_p \sim 2D$. Later on, a decrease of U_p occurs due to the piston deceleration and 2D effects. These effects have been assessed by the diagnostic TRANS by looking at $\sim$100–200 μm ahead of the foam surface. We get a shock front picture and its shape is not quite planar. Moreover, according to this system, the plasma width in the precursor is $d \sim 200$ μm. Since the shift depends also on the electron density per unit plasma length ($\approx 4.5 \times 10^{21}$ cm^{-3} μm^{-1}/fringe) we deduce $n_e(t)$; see Fig. 5.

Numerical simulations clearly show (see below) that the precursor is, in fact, an ionized zone where the plasma is at rest (the gas moves significantly only after the passage of the shock). The spatial profiles $n_e(x, t)$ at a given time can be derived using a reconstruction procedure from the interferograms. The deduced ionization wave velocity is 70 (130) km/s for isodensity contours $n_e = 10^{20}$ ($n_e = 10^{19}$) cm^{-3}. These results agree rather well with the values of U_p and D given above.

The formation of the precursor requires a careful numerical treatment of radiation transport with a very high spatial resolution. In order to estimate the nonequilibrium effects that govern the early propagation of the precursor, numerical simulations with $V_p = \text{const}$ driven SC shock have been performed with the radiative hydrocode ASTROLABE [26]. This fully implicit, moving grid code uses the two-moment radiative transfer approximation and takes into account non-local-thermal-equilibrium effects. With $V_p = 65$ km/s, the precursor plasma enters the RS with a 2 keV kinetic energy per ion and, according to the Xe-EOS, dissipation of this energy results in a plasma with a mean ionization equal to 15 with $T_2 =$ 32–37 eV for $\rho_1 = 10^{-3}$–10^{-2} g/cm^3.

Figure 6 displays the structure of the nonstationary RS in the vicinity of the discontinuity. The temperature in the dense shocked gas and in the precursor is $\sim$20 eV, i.e., less than 32 eV. The latter would be achieved only for a steady state. The sharp T_i spike at the shock front is specific to SC shocks. A moving grid numerical resolution of the spike shows that it consists in three zones, through which the gas compression rises up to a final value $\sim$55 (depending, actually, on the gas opacity). Shortly after the viscous shock high heating of the Xe ions (the end of this first step is shown by the X on the ρ curve; compression is 4), a first relaxation (second step) occurs with $T_i = T_e$. A second relaxation (third step) happens where matter thermal energy moves to photons on a distance shorter than λ until gas and radiation rise to the same temperature. This zone is the source of the radiative flux (shock luminosity) that heats the gas ahead of the shock and creates the precursor. Its length is $\sim$500 μm at $t = 5$ ns and cannot be shown in Fig. 6. Unfortunately, the experimental study of the spike properties is not yet possible with our detector capabilities.

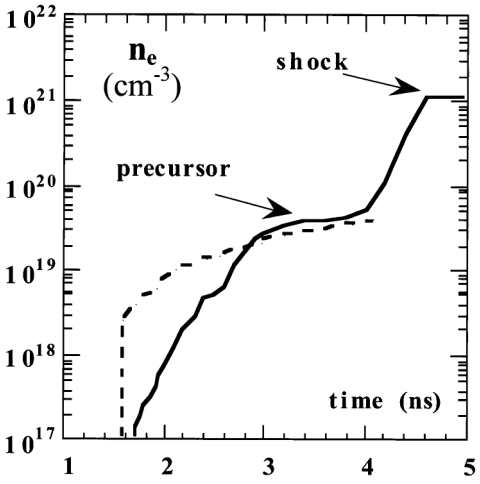

FIG. 5. Experimental and simulated values of n_e (dashed and solid curve, respectively) in xenon, 200 μm away from the foam surface.

Experiments have also been simulated with two more Lagrangian radiative 1D hydrocodes, MULTI [21] and FCI1 [22]. Both take into account the laser-matter interaction, the target design and a multigroup radiative transfer in the diffusion approximation. A detailed comparison (i.e., experiment versus computation) of the precursor dynamics is not easy because it depends upon the value of n_e which, in turn, depends on d (known to within about 20%). However, the similarity between the calculated and the observed precursor is rather promising (see Fig. 5). For example, 4 ns after the shock breakout in Xe gas, we get $U_p \sim 100$ km/s from TRANS (see Fig. 4) for the isovalue $n_e = 3 \times 10^{19}$ cm^{-3} and for $d =$ 200 μm. In the same conditions, MULTI (FCI1) gives 120 (300) km/s. These values have the same order of magnitude but the FCI1 one is overestimated. With $V_p =$ 65 km/s, ASTROLABE provides U_p that decreases with time from 170 to 130 km/s. At $t = 4$ ns, $U_p \sim 150$ km/s.

In conclusion, we have observed, at the LULI facility, the development of a radiative precursor ahead of a strong SC-RS in low pressure Xe gas. Using various diagnostics, the experimental results are in good agreement with numerical simulations. In particular, the measured value of D is very close to the numerical one. The experimental value of U_p remains within the range obtained with the three codes. This discrepancy shows that much theoretical and experimental work is required to get a better and more reliable model of RSs. The resolution of the diagnostics will be improved and multidimensional effects will be studied (hydrodynamics and radiative transfer). In the near future, the upgraded laser facility at LULI will allow one to explore the physics of stronger RSs.

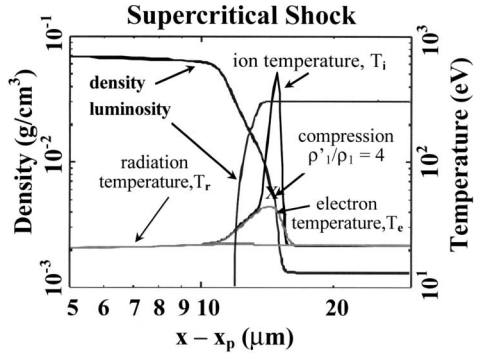

FIG. 6. Blowup of the SC-RS at $t = 5$ ns for a 65 km/s moving piston with position x_p. These results come from ASTROLABE for $\rho_1 = 1.3 \times 10^{-3}$ g/cm^3 and $T_1 = 300$ K.

The authors are grateful to B. Marchet, J. Grenier (CEA), and Ph. Moreau (LULI) for their significant contribution to the success of these experiments. We thank the target designer groups: F. Gex and P. Barroso (GEPI/Observatoire de Paris) and L. Polès, P. Sys, F. David, J. Tidu, P. Di Nicola, and B. Cathala (CEA). The authors acknowledge the Programme National de Physique Stellaire (CNRS), the Observatoire de Paris, and CEA for their financial support.

[1] D. Mihalas and B.W. Mihalas, *Foundations of Radiation Hydrodynamics* (Oxford University, Oxford, 1984).
[2] G.C. Pomraning, *The Equations of Radiation Hydrodynamics* (Pergamon, Oxford, 1973).
[3] Y. B. Zeldovich and Y. P. Raizer, *Physics of Shock Waves and High Temperature Hydrodynamic Phenomena* (Academic, New York, 1967).
[4] J. Lindl, Phys. Plasmas **2**, 3933 (1995).
[5] B. Remington *et al.*, Phys. Plasmas **7**, 1641 (2000).
[6] P. Drake *et al.*, Astrophys. J. **564**, 896 (2002).
[7] S. Bouquet *et al.*, Astrophys. J. Suppl. Ser. **127**, 245 (2000).
[8] D. R. Farley *et al.*, Phys. Rev. Lett. **83**, 1982 (1999).
[9] T. Ditmire *et al.*, Astrophys. J. Suppl. Ser. **127**, 299 (2000).
[10] A. Frank *et al.*, Astrophys. J. Lett. **494**, 79 (1998).
[11] S.V. Lebedev *et al.*, Astrophys. J. **564**, 113 (2002).
[12] A. Ciardi *et al.*, Laser Part. Beams **20**, 255 (2002).
[13] J. Grun *et al.*, Phys. Rev. Lett. **66**, 2738 (1991).
[14] M. J. Edwards *et al.*, Phys. Rev. Lett. **87**, 085004 (2001).
[15] J.-C. Bozier *et al.*, Phys. Rev. Lett. **57**, 1304 (1986).
[16] K. A. Keilty *et al.*, Astrophys. J. **538**, 645 (2000).
[17] X. Fleury *et al.*, Laser Part. Beams **20**, 263 (2002).
[18] P. A. Keiter *et al.*, Phys. Rev. Lett. **89**, 165003 (2002).
[19] K. Shigemori *et al.*, Astrophys. J. Lett. **533**, 159 (2000).
[20] M. Koenig *et al.*, Phys. Plasmas **6**, 3296 (1999).
[21] R. Ramis *et al.*, Comput. Phys. Commun. **49**, 475 (1988).
[22] R. Dautray and J.-P. Watteau, *La Fusion Thermonucléaire Inertielle par Laser* (Eyrolles, Paris, 1993).
[23] T. H. Bett *et al.*, Appl. Opt. **34**, 4025 (1995).
[24] M. Koenig *et al.*, Phys. Rev. E **50**, R3314 (1994).
[25] P. M. Celliers *et al.*, Appl. Phys. Lett. **73**, 1320 (1998).
[26] J.-P. Chièze *et al.* (private communication).